Materials Transactions, Vol. 48, No. 8 (2007) pp. 2043 to 2048
Special Issue on Crystallographic Orientation Distribution and Related Properties in Advanced Materials

Change in Microstructure and Texture during Annealing of Pure Copper Heavily Deformed by Accumulative Roll Bonding

Naoki Takata[1], Kousuke Yamada[2,*1], Ken-ichi Ikeda[3], Fuyuki Yoshida[3,*2], Hideharu Nakashima[3] and Nobuhiro Tsuji[1]

[1]*Dept. of Adaptive Machine Systems, Graduate School of Engineering, Osaka University, Suita 565-0871, Japan*
[2]*Dept. Molecular and Material Sciences, Interdisciplinary Graduate School of Engineering Science, Kyushu University, Kasuga 816-8580, Japan*
[3]*Faculty of Engineering Sciences, Kyushu University, Kasuga 816-8580, Japan*

Pure copper sheets were heavily deformed up to equivalent strain of 4.8 by the accumulative roll-bonding (ARB) processed and then annealed. The ARB processed copper showed the ultra-fine grained microstructure which consisted of relatively equiaxed grains having grain thickness of about 0.2 μm. The DSC measurement of the ARB processed specimens revealed that the recrystallization temperature significantly decreased with increasing the number of the ARB cycles. The stored energy did not increase so much at later stage of ARB, which corresponded with the change in microstructure. The recystallization behavior of the ARB processed copper was governed by discontinuous recrystallization characterized by nucleation and growth process. Remarkable development of cube texture ($\{100\}\langle001\rangle$) was found in the specimen deformed to the equivalent strain of 3.2 or larger and then annealed. The concentration of the cube recrystallization texture depended on the number of ARB cycles. [doi:10.2320/matertrans.MA200701]

(Received February 9, 2007; Accepted April 25, 2007; Published July 25, 2007)

Keywords: *severe plastic deformation, ultra-fine grains, recrystallization, stored energy, cube texture*

1. Introduction

The accumulative roll-bonding (ARB), which is one of the severe plastic deformation (SPD) processes, can make it possible to produce bulky sheets having ultra-fine grained (UFG) microstructures with mean grain size of less than 1 μm.[1–4] The UFG metallic materials perform strength much higher than that of the ordinary materials with coarse grain size of 10∼100 μm. Various SPD processes have been energetically studied to produce the UFG materials performing excellent mechanical properties. It has been recently revealed that the SPD processes can enhance not only the grain refinement but also the development of specific textures in various materials.[5–9] It is, thus, considered that the combination of SPD and annealing process has a potential for controlling not only grain size but also texture that cannot be obtained through conventional processes. Therefore, it is fundamentally important to clarify the recystallization behavior and texture development in annealing of the SPD processed materials. The annealing behavior of the ARB processed materials has been clarified in pure aluminum and low carbon steel which were so-called "recovery type" materials having high stacking fault energy or bcc structure.[10,11] However, the annealing behavior of the ARB processed materials having medium or low stacking fault energy has not yet been investigated. In the present study, the annealing behavior and texture development in copper ARB processed by various cycles were studied in detail by differential scanning calorimetry (DSC) analysis and electron back scatter diffraction pattern (EBSP) analysis.

2. Experimental

Oxygen-free 99.99% purity copper sheets were used in the present study. The starting sheets had fully recrystallized microstructure with mean grain size of 7.7 μm. The copper sheets, of which dimensions were 1 mm thick, 20 mm wide and 335 mm long, were provided for the ARB process at room temperature without lubrication.[1–4] The ARB process was carried out to various cycles, *i.e.*, to equivalent strains of 1.6 (2 ARB cycles), 3.2 (4 ARB cycles) and 4.8 (6 ARB cycles). The deformation microstructure was investigated by EBSP analysis in a field emission type scanning electron microscope (FE-SEM) HITACHI S-4300SE operated at 20 kV and also by transmission electron microscopy (TEM) using JEOL JEM-2000EX operated by 200 kV. The specimens deformed by various ARB cycles were annealed at 150°C for various periods ranging from 60 to 36000 s under a vacuum condition of 10^{-3} Pa. The annealed microstructures were characterized by EBSP using a W-filament SEM (JEOL JSM-5310) operated at 25 kV. The samples for the observation were prepared by mechanical polishing and twin-jet electropolishing in a solution of phosphoric acid and water of 7 : 3 ratio in volume. Microstructure was observed from the transverse direction (TD) of the sheets.

In order to investigate the thermal behavior during the annealing, DSC curves of the ARB processed specimens were measured using RIGAKU Thermo Puls2 DSC system. The DSC measurements were carried out at a heating rate of 0.67°C/s in an inert atmosphere with high purity Ar gas.

Vickers hardness of the specimens was measured using Akashi AVK-C100 Hardness Tester. The indentation test was carried out with the load of 2.94 N for 15 seconds.

*1Graduate Student, Kyushu University (Present address: Fuji Heavy Industries, Ltd.)
*2Present address: Nakayama Steel Works, Ltd., Osaka 511-8551, Japan

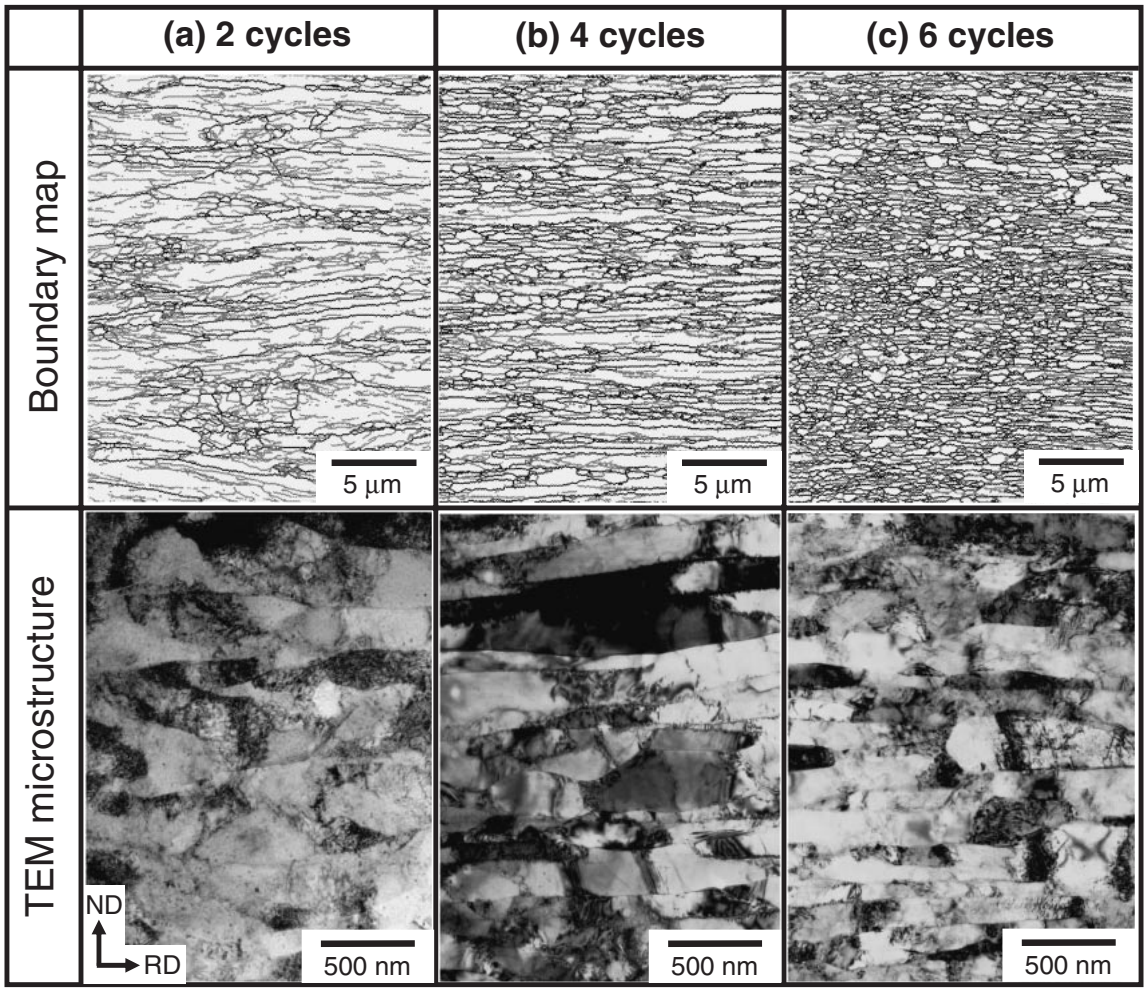

Fig. 1 Boundary maps and TEM microstructures of the copper specimens ARB processed by various cycles. In boundary maps, gray lines represent the misorientation (θ) of $2^\circ \leq \theta < 15^\circ$, while black lines represent $15^\circ \leq \theta$.

3. Results and Discussion

3.1 Microstructure

Figure 1 shows both the boundary maps obtained from the EBSP analysis and the TEM microstructures of the copper specimens ARB processed by (a) 2 cycles, (b) 4 cycles and (c) 6 cycles. The boundary maps were measured at the thickness locations of $t/t_0 = 0.1$ (t: distance along normal direction (ND) from the center, t_0: total thickness of the sheet). In the maps, black lines indicate high angle boundaries whose misorientation is larger than 15 degrees, while gray lines indicate low angle boundaries with misorientation ranging from 2 degrees to 15 degrees. Here the misorientation smaller than 2 degrees was cut off in order to remove the inaccuracy in the EBSP measurement and analysis.[12] The specimen ARB processed by 2 cycles showed somewhat inhomogeneous microstructure composed of the initial grains elongated to the rolling direction (RD), which was a typical deformation microstructure. TEM microstructures clearly show the elongated dislocation substructures involving tangled dislocations and dislocation cells. These correspond to the low angle boundaries detected by the EBSP measurement. In the EBSP maps, several small regions surrounded by high angle boundary could be also observed at the vicinity of initial grain boundaries. The 4-cycle specimen showed elongated microstructure finely subdivided by high angle boundaries along ND. After 4 cycles, the microstructure became rather homogenous and the fraction of high angle boundary greatly increased. The TEM observation revealed that the contour of grain boundaries could be clearly recognized in the 4-cycle specimen. It is also noteworthy that the dislocation density within the cell or ultrafine grains seems rather deceased. These results indicate that low angle boundaries that consist of accumulated dislocations change into sharp boundaries with larger misorientation during the ARB. The microstructure of the 4-cycle specimen is similar to the so-called "lamellar boundary structure" which has been reported in the heavily rolled materials.[13] In contrast, several rather equiaxed grains could be also observed together with the lamellar boundary structure, as shown in the EBSP map. The equiaxed grains suggest the occurrence of partial recrystallization during the ARB. The 6-cycle specimen shows fine microstructure that consisted of relatively equiaxed grains, which is different from that of the 4-cycle specimen in morphology. It should be noted that some coarse grains with grain size of several micrometers could be observed in the UFG microstructure of the 6-cycle specimen. These coarse grains represent that recovery and recrystalli-

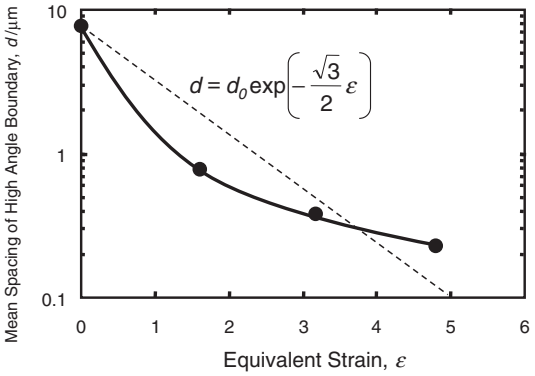

Fig. 2 Change in mean spacing of high angle boundaries in the ARB processed copper as a function of equivalent strain. A broken line indicates geometrically expected thickness of the initial grains (d) calculated from the total strain (ε) and initial grain size (d_0) according to the attached equation.

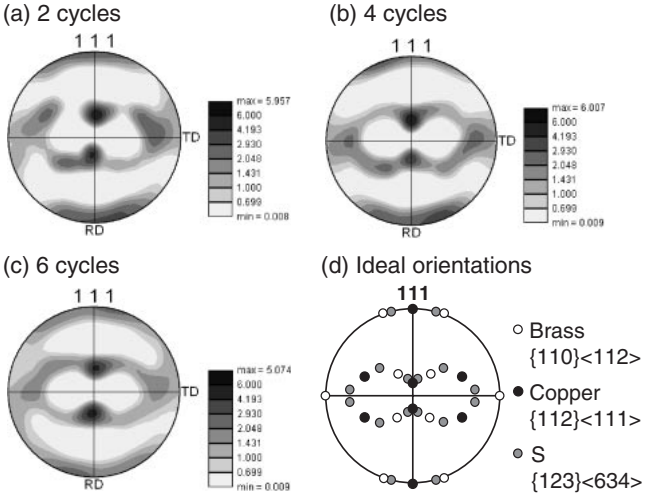

Fig. 3 (111) pole figures of the copper specimens ARB processed by 2 cycles (a), 4 cycles (b) and 6 cycles (c). The pole figure of the ideal orientation of the b-fiber texture components in rolled fcc metals is shown in (d).

zation take place during the ARB. The reason for the occurrence of recrystallization at low temperature will be discussed later.

Figure 2 shows the change in the mean spacing of high angle boundaries during the ARB. The spacing was measured along ND in the EBSP boundary maps. In Fig. 2, geometrically expected thickness of the initial grains (d) calculated from the total strain (ε) and initial grain size (d_0) was superimposed as a broken line. The measured spacing greatly decreased below 1 μm by 2 ARB cycles. The measured thickness was much smaller than the expected thickness of the initial grains. This means that a large amount of high angle boundaries are newly formed within the initial grains during the plastic deformation. Such a microstructure evolution process is called "grain subdivision", which has been confirmed in deformed fcc metals and alloys.[13] As the deformation progressed, the mean thickness decreased furthermore, which reached to 0.23 μm after 6 cycles. However, the rate of grain refinement reduced with increasing the total strain. The measured thickness became even coarser than that of the expected thickness after 6 cycles. This suggests that any process of microstructure coarsening happens in the material during the ARB process. One of the possible reasons for coarsening is the occurrence of partial recrystallization during the ARB. Previous studies have also revealed that recrystallization locally happened in high purity copper even if the ARB process was carried out at ambient temperature.[14,15] The possible reasons for the occurrence of recrystallization at such a low temperature are as follows: (i) heat generation due to large plastic deformation, (ii) decrease in recrystallization temperature caused by increase in lattice defects introduced during severe plastic deformation, and (iii) high purity (99.99%) of the present copper. It is known that most of plastic working energy turn to heat. Actually, it has been reported that the temperature of commercial purity aluminum sheets rose up to approximately 200°C during the ARB conducted at room temperature.[16] Furthermore, the UFG microstructure fabricated by the ARB contains a large driving force to coarsen because of its high density of dislocations and grain boundaries. Additionally, it can be considered that high purity of the present material assists the microstructure coarsening even at relatively low temperature. The recrystallization during the ARB is therefore considered to be essentially the same as conventional discontinuous recrystallization that can be observed at high temperature in heavily rolled copper.

Figure 3 shows {111} pole figures obtained from the EBSP analysis of the copper specimens ARB processed by various cycle. The ARB processed copper had typical rolling texture with β-fiber components. The pole figure showing the ideal orientation of the β-fiber texture components in rolled fcc metals composed of so-called Brass $\{110\}\langle 112\rangle$, Copper $\{112\}\langle 111\rangle$ and S $\{123\}\langle 634\rangle$ is shown in Fig. 3(d). In this figure, white, black and gray symbols correspond the Brass, the Copper and the S orientations, respectively. The concentration of $\{110\}\langle 112\rangle$ (Brass) decreased with increasing the equivalent strain, while $\{112\}\langle 111\rangle$ (Copper) remained in high intensity in the 6-cycle specimen. Such a texture development is similar to the conventionally rolled copper.[17] However, the maximum intensity of pole figures slightly decreased after 6 cycles. This result indicated that texture became somewhat random by 6 cycles ARB. This is probably a characteristic of the ARB processed materials. It can be considered that the randomization is attributed to the complicated introduction of large redundant shear strain caused by the friction between the rolls and sheets in the non-lubricated ARB process.[2,18]

3.2 Change in stored energy

Figure 4 shows the DSC curves of the copper specimens ARB processed by various cycles. The exothermic peaks appeared in the ARB processed copper. The microstructural observation of the specimens before and after the DSC measurements confirmed that these peaks corresponded with recrystallization. The peak positions clearly shifted to lower temperature with increasing the number of ARB cycles, which indicated that recrystallzaition was greatly enhanced by ultra-high straining. Assuming the released energy

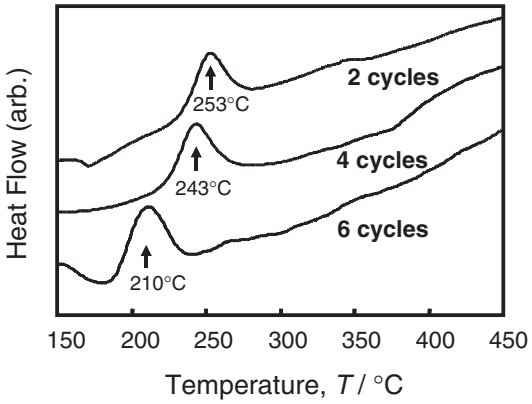

Fig. 4 DSC curves of the copper specimens ARB processed by various cycles measured at a heating rate of 0.67°C/s.

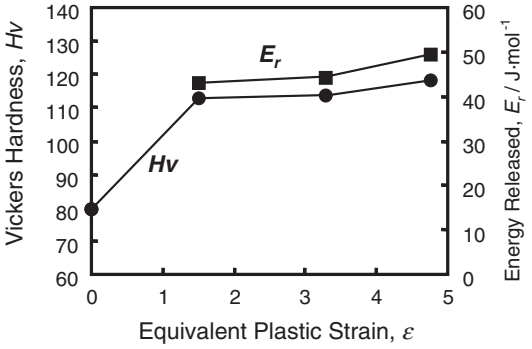

Fig. 5 Vickers hardness and released energy obtained form the DSC measurements of the copper specimens ARB processed by various cycles.

corresponded to the stored energy in the material, the release energy was calculated from the exothermal peaks for evaluation of the stored energy accumulated by the ARB. The released energy and Vickers hardness of the ARB processed specimens are shown in Fig. 5. The stored energy (released energy) significantly increased by 2 ARB cycles and then slightly increased with increasing the equivalent strain. The change of the Vickers hardness synchronized well with the change of the stored energy. These results prove that the stored energy dose not change so much at later stage of the ARB process in spite of the progress of the lattice defect accumulated. We should take account of the microstructural change during the ARB for understanding the conflict between the substantially constant stored energy and the decrease in recrystallization temperature. The EBSP and TEM observations revealed that sharp boundaries with large misorientation displaced irregular shaped boundaries composed of high dense dislocations in the later stage of the ARB. This indicates that the accumulated dislocations are rearranged and turned into high angle grain boundaries, which results in the saturation (or rather decrease) of dislocation density within the microstructure. Thus, it can be assumed that the rearrangement and transformation of accumulated lattice defect is the reason for the saturated stored energy. Additionally, the partial recrystallization happened during the ARB can be considered as a minor contribution for the annihilation in dislocation. In contrast, the density of high angle boundary significantly increased with increasing the number of ARB cycle. It is well known that high angle boundaries exhibit higher mobility for grain boundary migration than low angle boundaries. Therefore, the increase in high angle boundary can enhance the grain boundary migration at lower temperature, resulting in the lowering recrystallization temperature in the DSC curves.

3.3 Recrystallization texture

Figure 6 shows the orientation color maps and (111) pole figures obtained from EBSP analysis of the copper specimens ARB processed by various cycles and then subsequently annealed at 150°C for 1800 s. In these maps, the color represents the ND orientation of each region according to the orientation color key in unit triangle shown in Fig. 6. The microstructural change during the annealing was the typical discontinuous recrystallization characterized by nucleation and growth of coarse grains.[19] Such an annealing process of the ARB processed copper having relatively low stacking fault energy is different from that in aluminum or ferritic steel[4,5] which are categorized as so-called "recovery type" materials. Figure 6 clearly shows that the recrystallization texture changes depending on the number of ARB cycles. The 2-cycle specimen showed fully recrystallized microstructure with mean grain size of 36 μm after annealing, which had rather random texture remaining a trace of as-deformed texture. However, the remarkable development of cube texture ($\{100\}\langle001\rangle$) was observed in the specimens heavily deformed over the equivalent strain of 3.2 (above 4 ARB cycles). The recrystallized cube grains were much coarser than other recrystallized grains in the 4- and 6-cycle specimens. The development of cube texture occurred through the preferential growth of the cube grains consuming the deformation microstructure during the primary recrystallization. The pole figures also show the intensity of the twin related orientation to the cube orientation in the 4 and 6-cycle specimens. The EBSP maps show that there are a large number of annealing twins in the coarse cube grains. These indicate that the preferential growth of cube grain comes along with the formation of high dense annealing twins.

Figure 6 also shows the intensity of cube texture depends on the number of the ARB cycles. The pole figures clearly represent that the annealed 4-cycle specimen has sharper cube texture than the 6-cycle specimen. Here, the possible reasons for the difference of texture intensity are discussed. Some of the present authors have investigated the optimum condition of the thermo-mechanical treatment for sharp cube texture formation in pure aluminum foils.[20,21] These studies have revealed that the volume fraction of recrystallized cube grains increased with increasing the volume fraction and the number of the cube-oriented regions in the as-deformed state. This result confirmed that the development of cube texture during an annealing was significantly influenced by the distribution of potential cube nuclei in the deformed materials. Thus, the volume fraction of cube-oriented regions in the present copper specimen ARB processed by various cycles was similarly investigated through the thickness of the sheets. The result is shown in Fig. 7. In this figure, the thickness locations are expressed using the ratio of the distance along ND from the center, t, and thickness of the sheet, t_0. That is, $t/t_0 = 0$ and $t/t_0 = 0.5$ correspond to the

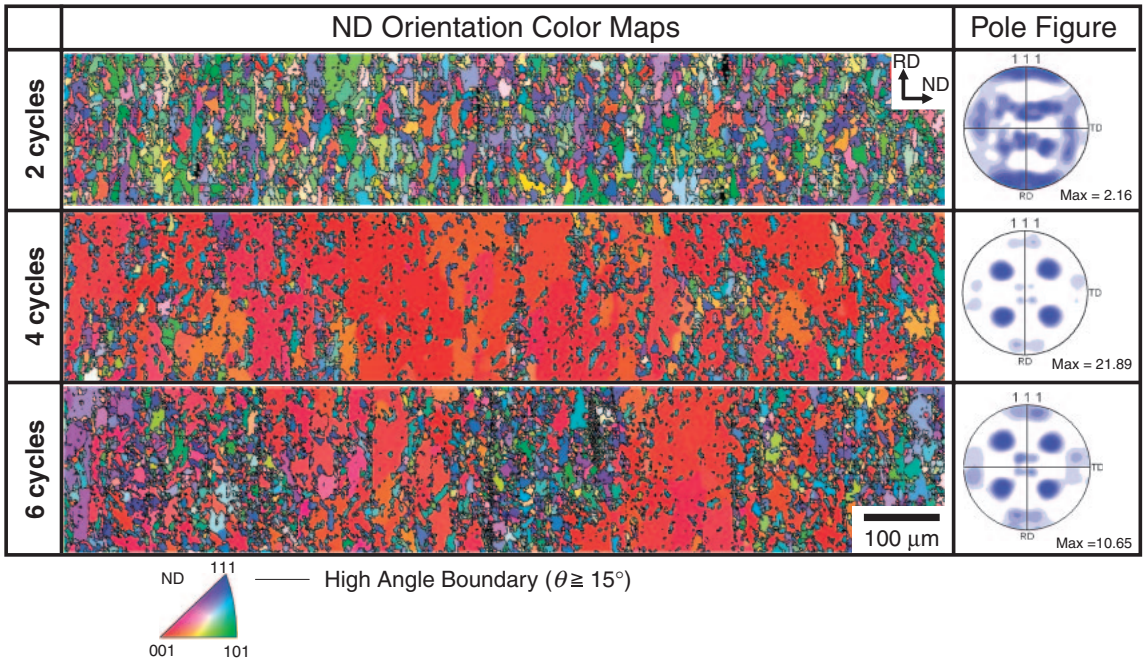

Fig. 6 ND orientation color maps and (111) pole figures obtained from the EBSP measurements in the copper specimens ARB processed by various cycles and subsequently annealed at 150°C for 1800 s. The maps were obtained from the measurements throughout the thickness of sheets.

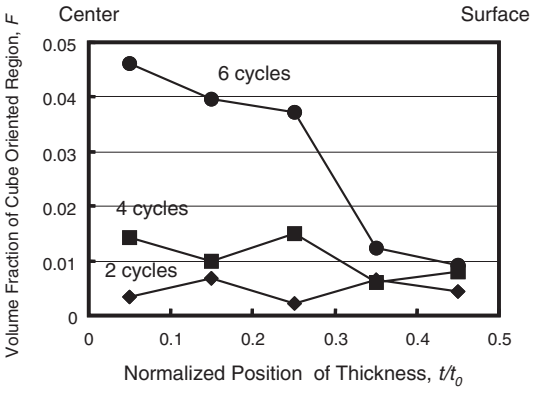

Fig. 7 Distribution of cube-oriented regions through thickness in the copper specimens ARB processed by various cycles.

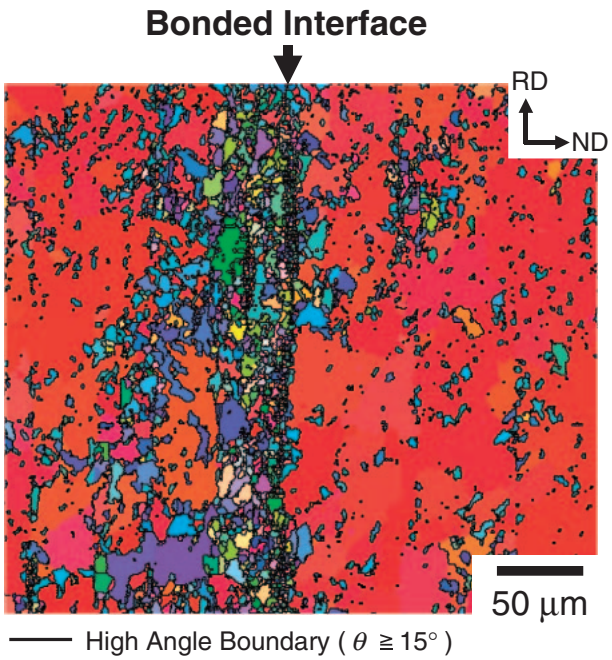

Fig. 8 Orientation color map showing recystallized microstructure in the vicinity of a bonded interface in copper specimens ARB processed by 6 cycles and subsequently annealed at 150°C for 600 s. The color represents the ND orientation of each region according to the orientation color key in unit triangle shown in Fig. 6.

thickness center and one surface, respectively. The volume fraction of cube-oriented regions increased with increasing the number of the ARB cycles at every thickness location. The volume fraction of cube-oriented regions was limited below 1% in the 2-cycle specimen. Larger fraction of cube grains distributed in the center regions than surface regions in the 4 and 6-cycle specimens. The smaller fraction of cube-oriented regions at the surface of the 6-cycle specimen is probably due to large shear deformation at subsurface regions caused by the friction between the rolls and material.[2,18] It can be therefore considered that the 2-cycle specimen has insufficient number of cube nuclei for the development of sharp cube texture, which results in the rather random texture after the annealing.

It was mentioned that the 6-cycle specimen revealed lower intensity of cube texture than that of the 4-cycle specimen after the annealing. In contrast, the density of cube-oriented regions in the as-ARB state was higher in the 6-cycle specimen than in the 4-cycle specimen. This conflict means that there are another factors to control the cube texture development in the ARB processed copper. Figure 8 shows the orientation color map in the vicinity of bonded interface of the 6-cycle specimen annealed at 150°C for 300 s. The recrystallized microstructure consisted of not only the coarse cube grains but also many fine grains. A large amount of

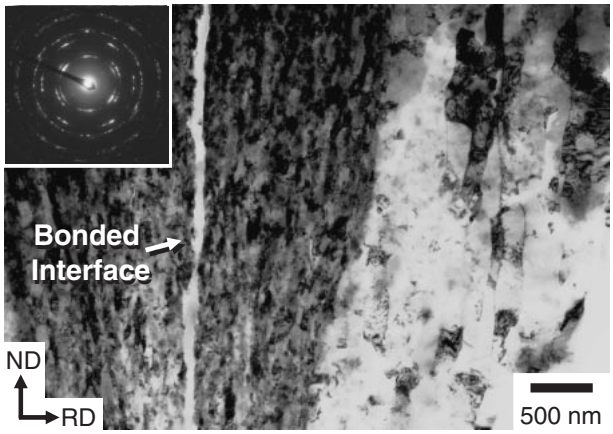

Fig. 9 TEM image showing the nanocystalline structure in the vicinity of a bonded interface in the copper specimen ARB processed by 6 cycles.

recrystallized grains with several micrometers formed around the bonded interface and they had various orientations. The minute EBSP measurement revealed that the recrystallization behavior in the vicinity of the bonded interface is different from that of the sheets interior. It can be considered that the formation of fine recrystallized grains around the bonded interface weakens the intensity of developed cube texture. One of the reasons for the formation of the fine recystallized grains should be the redundant shear deformation introduced at subsurface regions in every ARB cycle. The half of the sheared subsurface regions becomes the bonding interface in the next ARB cycle, and the large shear strain and shear texture would produce the fine recrystallized grains with orientations different from those at sheet interior. Additionally, there seems another reason for the fine grain formation around the bonded interface. Figure 9 shows a TEM microstructure in the vicinity of a bonded interface in the 6-cycle specimen. The region in vicinity of the bonded interface showed much finer grained-structure than the sheet interior. The mean grain size reached to 70 nm. It has been reported that the wire-brushing in the ARB process acted as a kind of SPD to form the nanocystalline layers.[22] As the number of the bonded interfaces increases with increasing the number of the ARB cycles, the recrystallization behavior would be more scattered by the nanocrystalline interface regions having particular microstructure in the material processed by higher ARB cycles. Additionally, fine oxide particles introduced at bonded interfaces during wire-brushing might show a pining effect on grain boundary migration to inhibit the development of cube texture.

4. Summary

The characteristics of the pure copper sheets severely deformed by the ARB process and then annealed were investigated. The key results are summarized as follows:
(1) The ARB processed copper showed the UFG microstructure that consisted of relatively equiaxed grains whose grain size was about 0.2 μm. The stored energy introduced by high straining did not increase so much in the later stage of the ARB, which was likely to relate to the rearrangement and transformation of the accumulated lattice defects during the SPD.
(2) Remarkable development of cube texture ($\{100\}\langle001\rangle$) was observed in the annealed copper ARB processed above 4 cycles (equivalent strain of 3.2). The cube texture developed through the preferential growth of cube grains during primary recyrstallzaiton. The concentration of cube texture depended on the number of ARB cycles.

Acknowledgements

The authors would like to express hearty thank to Professor Hiroshi Abe (Kyushu University) for fruitful advice and discussions. This study was supported by a Grant-in-Aid for scientific research from the ministry of education, culture, sports, science and technology (MEXT), Japan, on priority areas “Giant straining process for advanced materials containing ultra-high density lattice defects”.

REFERENCES

1) *SEVERE PLASTIC DEFORMATION*, Towards Bulk Production of Nanostructured Materials, edited by B. S. Altan, I. Miskioglu, G. Purcek, R. R. Mulyukov and R. Artan, (NOVA Science Publishers, New York, 2006).
2) N. Tsuji, Y. Saito, S. H. Lee and Y. Minamino: Adv. Eng. Mater. **5** (2003) 338–342.
3) Y. Saito, H. Utsunomiya, N. Tsuji and T. Sakai: Acta Mater. **47** (1999) 579–583.
4) Y. Saito, N. Tsuji, H. Utsunomiya, T. Sakai and H. G. Hong: Srcipta. Mater. **39** (1998) 1221–1227.
5) O. V. Mishin and G. Gottstein: Phil. Mag. A **78** (1998) 373–388.
6) X. Huang, N. Tsuji, N. Hansen and Y. Minamino: Mater. Sci. Eng. A **340** (2003) 265–271.
7) N. Kamikawa, N. Tsuji and Y. Minamino: Sci. Tec. Adv. Mater. **5** (2004) 163–172.
8) A. Vinogradov, T. Ishida, K. Kitagawa and V. I. Kopylov: Acta Mater. **53** (2005) 2181–2192.
9) S. Li, A. A. Gazder, I. J. Beyerlein, E. V. Pereloma and C. H. J. Davies: Acta Mater. **54** (2006) 1087–1100.
10) N. Tsuji, Y. Ito, Y. Saito and Y. Minamino: Scripta Mater. **47** (2002) 893–899.
11) N. Tsuji, N. Kamikawa and Y. Minamino: Mater. Sci. Forum **467–470** (2004) 341–346.
12) N. Kamikawa, N. Tsuji, X. Huang and N. Hansen: Acta Mater. **54** (2006) 3055–3066.
13) N. Hansen and J. D. Jensen: Phil. Trans. R. Soc. Lond. A **357** (1999) 1447.
14) B. L. Li, N. Kamikawa and N. Tsuji: Mater. Sci. Eng. A **423** (2006) 331–342.
15) B. L. Li, N. Shigeiri, N. Tsuji and Y. Minamino: Mater. Sci. Fourm **503–504** (2006) 615–620.
16) N. Tsuji, T. Toyoda, Y. Minamino, Y. Koizumi, T. Yamane, M. Komatus and M. Kiritani: Mater. Sci. Eng. A **350** (2003) 108–116.
17) J. Hirsch and K. Lucke: Acta metall. **11** (1988) 2863–1882.
18) S. H. Lee, Y. Saito, N. Tsuji, H. Utsunomiya and T. Sakai: Scripta Mater. **46** (2002) 281–285.
19) F. J. Humphreys and M. Hatherly: *RECRYSTALLIZATION and Related Annealing Phenomena* (Pergamon, New York, 1995), p. 3.
20) K. Ikeda, N. Takata, F. Yoshida, H. Nakashima and H. Abe: Mater. Sci. Forum **396–402** (2002) 569–574.
21) N. Takata, K. Ikeda, F. Yoshida, H. Nakashima and H. Abe: J. JILM **53** (2003) 218–223.
22) M. Sato, N. Tsuji, Y. Minamino and Y. Koizumi: Sci. Tec. Adv. Mater. **5** (2004) 145–150.